AFRL-PR-WP-TM-2003-2044

MIXING AND PROCESSING OF COMPLEX BIOLOGICAL FLUIDS

Dorian Liepmann

University of California at Berkeley
Sponsored Projects Office
336 Sproul Hall
Berkeley, CA 94720-5940

MARCH 2003

Final Report for 01 September 1998 – 01 January 2002

PROPULSION DIRECTORATE
AIR FORCE RESEARCH LABORATORY
AIR FORCE MATERIEL COMMAND
WRIGHT-PATTERSON AIR FORCE BASE, OH 45433-7251

NOTICE

USING GOVERNMENT DRAWINGS, SPECIFICATIONS, OR OTHER DATA INCLUDED IN THIS DOCUMENT FOR ANY PURPOSE OTHER THAN GOVERNMENT PROCUREMENT DOES NOT IN ANY WAY OBLIGATE THE US GOVERNMENT. THE FACT THAT THE GOVERNMENT FORMULATED OR SUPPLIED THE DRAWINGS, SPECIFICATIONS, OR OTHER DATA DOES NOT LICENSE THE HOLDER OR ANY OTHER PERSON OR CORPORATION; OR CONVEY ANY RIGHTS OR PERMISSION TO MANUFACTURE, USE, OR SELL ANY PATENTED INVENTION THAT MAY RELATE TO THEM.

THIS REPORT IS RELEASABLE TO THE NATIONAL TECHNICAL INFORMATION SERVICE (NTIS). AT NTIS, IT WILL BE AVAILABLE TO THE GENERAL PUBLIC, INCLUDING FOREIGN NATIONS.

THIS TECHNICAL REPORT HAS BEEN REVIEWED AND IS APPROVED FOR PUBLICATION.

KIRK L. YERKES
Research Engineer
Energy Storage & Thermal Sciences Branch

JOHN K. ERBACHER
Acting Chief
Energy Storage & Thermal Sciences Branch

JOSEPH A. WEIMER
ACTING CHIEF
POWER DIVISION, AFRL/PRP

Do not return copies of this report unless contractual obligations or notice on a specific document requires its return.

REPORT DOCUMENTATION PAGE

Form Approved
OMB No. 0704-0188

1. REPORT DATE *(DD-MM-YY)*	2. REPORT TYPE	3. DATES COVERED *(From - To)*
March 2003	Final	09/01/1998 – 01/01/2002

4. TITLE AND SUBTITLE
MIXING AND PROCESSING OF COMPLEX BIOLOGICAL FLUIDS

5a. CONTRACT NUMBER
N/A

5b. GRANT NUMBER
F33615-98-1-2910

5c. PROGRAM ELEMENT NUMBER
69199F

6. AUTHOR(S)
Dorian Liepmann

5d. PROJECT NUMBER
ARPP

5e. TASK NUMBER
98

5f. WORK UNIT NUMBER
03

7. PERFORMING ORGANIZATION NAME(S) AND ADDRESS(ES)

University of California at Berkeley
Sponsored Projects Office
336 Sproul Hall
Berkeley, CA 94720-5940

8. PERFORMING ORGANIZATION REPORT NUMBER
25313-23795-44-NDDXL

9. SPONSORING/MONITORING AGENCY NAME(S) AND ADDRESS(ES)

Propulsion Directorate
Air Force Research Laboratory
Air Force Materiel Command
Wright-Patterson Air Force Base, OH 45433-7251

10. SPONSORING/MONITORING AGENCY ACRONYM(S)
AFRL/PRPS

11. SPONSORING/MONITORING AGENCY REPORT NUMBER(S)
AFRL-PR-WP-TM-2003-2044

12. DISTRIBUTION/AVAILABILITY STATEMENT
Approved for public release; distribution is unlimited.

13. SUPPLEMENTARY NOTES

14. ABSTRACT

The primary deliverables for this research project have been the ability to predict the characteristics of the flow of complex biological fluids, including viscoelastic fluids and blood, and the effect of microfluidic control on the makeup and molecular structure of biological fluids. For this project, we focused on two critical fluids that are biologically significant and that are of critical importance to DoD: DNA-laden fluids for early identification and diagnosis of pathogens, and blood for on-field reconstitution of whole blood from stabilized components. In addition to experimental investigations of complex fluid flows, computational and modeling capabilities have also been developed. The experimental results have been used to validate modeling tools at both Berkeley/LBL and at CFD Research Corporation. New capabilities for BioMEMSdesign have been added to the commercial computational tools available from CFD Research Corporation as a result of this project.

15. SUBJECT TERMS
rheology, DNA laden flows, blood flow, microdevice, MEMS, microfluidics

16. SECURITY CLASSIFICATION OF:			17. LIMITATION OF ABSTRACT:	18. NUMBER OF PAGES	19a. NAME OF RESPONSIBLE PERSON (Monitor)
a. REPORT	b. ABSTRACT	c. THIS PAGE			Kirk Yerkes
Unclassified	Unclassified	Unclassified	SAR	18	19b. TELEPHONE NUMBER *(Include Area Code)* (937) 255-5721

Standard Form 298 (Rev. 8-98)
Prescribed by ANSI Std. Z39-18

Final Report

Mixing and Processing of Complex Biological Fluids

Contract Number: F33615-98-1-2910

Dorian Liepmann

UC Berkeley

The primary deliverables for this research project have been the ability to predict the characteristics of the flow of complex biological fluids, including viscoelastic fluids and blood, and the effect of micro-fluidic control on the make-up and molecular structure of biological fluids. For this project we focused on two critical fluids that are biologically significant and that are of critical importance to DOD: DNA-ladened fluids for early identification and diagnosis of pathogens and blood for on-field reconstitution of whole blood from stabilized components. In addition to experimental investigations of complex fluid flows, computational and modeling capabilities have also been developed. The experimental results have been used to validate modeling tools at both Berkeley/LBL and at CFD Research Corporation. New capabilities for BioMEMSdesign have been added to the commercial computational tools available from CFD Research Corporation as a result of this project. Specific developments and results are described below.

Experimental Investigation of DNA-Ladened Fluids

Inherent in microfluidic systems is the potential for parallel processing and high throughput analyses, improved sensitivity in particle detection, process automation, and increased cost efficiency. Already researchers have demonstrated use of microsystems for performing multiple biochemical protocols including capillary electrophoresis, cell fractionation, DNA sequencing, electrochromatography, and polymerase chain reaction (PCR). A complementary area of research is the design and fabrication of components intended to facilitate these processes. The intent of this work is to bridge the gap between these two areas of research and to focus on the behavior of biological macromolecules flowing through microfluidic devices. Of particular interest is the effect of flow and device geometry on macromolecular transport and conformation. Correlating microfluidic parameters and device geometries with macromolecular behavior enables improvements in the design and efficiency of micro total analysis systems intended for biochemical processing. Accordingly, the flow of λ-DNA solutions having varying concentrations and viscosities has been studied through geometries likely to comprise an actual microsystem: straight channels, sudden contractions, sudden expansions, and a micro check valve.

Straight channels and planar micro check valves were fabricated from silicon. Photolithography techniques were employed to transfer patterns from masks to the wafer surface. Using either thermally grown oxide or photoresist as a masking layer, a reactive ion etch (RIE) allowed definition of device feature depth. A more inclusive description of

the fabrication process for the microfluidic straight channel device appears in Shrewsbury, [1], and that for the micro check valve appears in Deshmuck [2].

Epifluorescence microscopy was used to visualize λ-DNA molecules. The molecules were labeled with the fluorescent dye YOYO-1 at a base pair:dye ratio of 5:1. In all experiments, λ-DNA was diluted to the specified concentration in a buffer solution containing 10 mM tris-HCl, 2 mM EDTA, 10 mM NaCl, and 4% β-mercaptoethanol. Bulk solution viscosities were increased as noted using sucrose. An Olympus IX70 inverted epifluorescence microscope equipped with a mercury burner served as the illumination source. A fluorescence cube having the following optical characteristics was used with the probe YOYO-1: excitation 460–500 nm, long pass beamsplitter 505 nm, emission 510-560 nm. The microscope was coupled to a Videoscope International high-gain image intensifier and a Cohu high performance monochrome CCD camera. All data were recorded to video. The data were transferred to a Macintosh G3 and analyzed using a Scion framegrabber and NIH Image software.

]The scanning electron micrograph in Fig. 1 illustrates the geometry of the microfluidic channel. The channel is 300 μm wide (in z), 60 μm deep (in y), and 8000 μm long (in x). Both ends of the channel terminate at two identical reservoirs. Fluid enters and exits the device by passing through holes located in these reservoirs. An important feature of the device is the narrowing of the fluidic path from the reservoir into the channel. This contraction produces an elongational flow.

The experiments were conducted to understand how macromolecules behave in a general microfluidic flow, a 0.3 μg/ml solution of λ-DNA molecules was visualized at 100X magnification flowing through the center of a microfluidic channel. In order to avoid entrance effects, the imaging location was placed downstream of the channel entrance, at a distance approximately equal to 1/3 the total channel length. Two solution viscosities (η = 1 cpoise, 25 cpoise) were studied at three flow rates (10 μl/hr, 20 μl/hr, 30 μl/hr). Fluorescent beads were imaged under identical experimental conditions to verify the absence of optical artifacts, stemming from limitations in the camera capture rate, in the recorded images. Sample λ-DNA images from the experiment for η = 25 cpoise appear in Fig. 2.Also shown are the maximum Deborah numbers (De) for the given set of experimental conditions. Here,

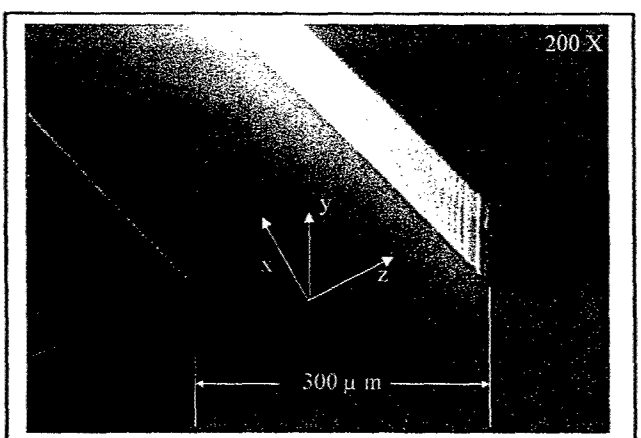

Fig. 1: SEM of Microfluidic Channel

$$De = \gamma\lambda \qquad (1)$$

where γ is the shear rate at the wall and λ is the relaxation time of λ-DNA molecules, as experimentally determined from rheological measurements (see Shrewsbury et al. for details).

The λ-DNA molecules in the 1 cpoise solution (not shown) seemingly elongate along streamlines at increasing flow rates and De numbers. A comparison of these images to beads, however, reveals that optical streaking obscures any stretching, as the beads mirror the pattern of the DNA. Thus, to continue pursuing this method of investigation, the solution viscosity, in lieu of shear rate, was increased in order to impose greater stress on the molecules but without altering the flow rate. As reflected in Fig. 2, the conformational changes in the λ-DNA for the 25 cpoise solution were striking. Increasing the solvent viscosity increased the relaxation time of the molecule, and dramatic changes in conformation could be observed at flow rates where streaking is negligible. Compare, for example, the images in Fig. 2 of the beads and of the DNA at a flow rate of 20 µl/hr. A histogram analysis recording the length distribution of a minimum of 100 molecules at each flow rate was conducted. The analysis (histograms not shown) indicates that a broad range of molecular conformations exists at all flow rates, and that molecular stretching is non-monotonic with flow rate.

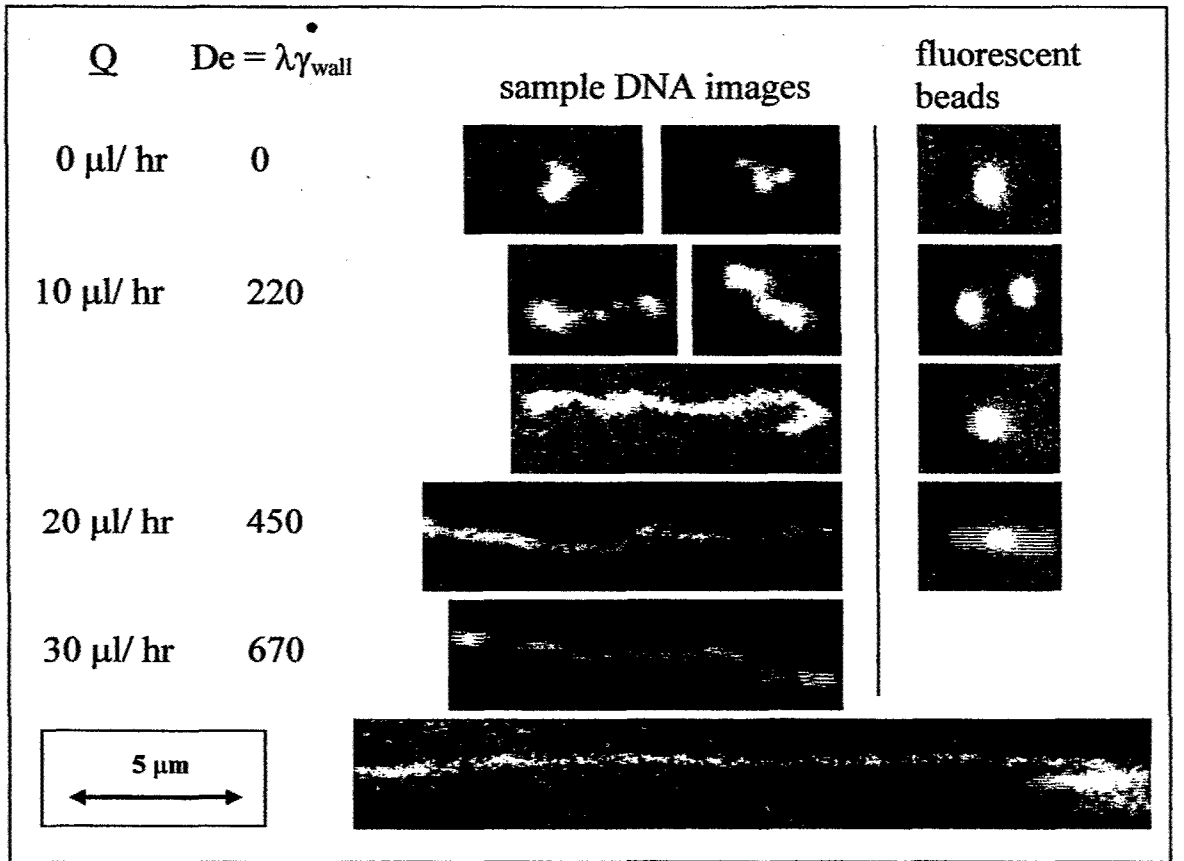

Fig. 2: λ-DNA Images along Channel Centerline (η = 25 cpoise)

The molecular deformation observed may be attributable to a combination of an elongational and a shear flow. At the channel centerline, the shear rates should be extremely low and, at the imaging location, the elongation channel entrance effects should have partially dissipated. Thus, two experiments to elucidate the relative contribution of each flow type to the observed effects logically follow. The first experiment examines an elongational flow along the channel centerline, and the second explores the shear flow at the channel wall.

An elongational flow exists at the channel centerline; the fluid accelerates as it enters the channel from the upstream reservoir and decelerates as it exits the channel into the downstream reservoir. Therefore, imaging DNA molecules moving through the centerline of the device lends insight into the impact of a converging and diverging flow in molecular conformation and identifies the positions within the device most likely to produce deformation of molecules. By using the fine focus of the microscope to locate the top and then bottom of the device (approximately 0.6 μm/division), the channel centerline was found. As illustrated in Fig. 3, the imaging position varied along x, the direction of flow, while the y and z positions remained constant. The concentration of DNA in buffered solution was 0.3 μg/ml, the viscosity was 15 centipoise, and the flow rate was 5 μl/hr.

At **A**, the DNA molecule is in the device reservoir. The shape, as represented by the representative sample images in Fig. 3, is coiled. Having fully entered the channel at **B** and having just undergone a converging flow, the DNA molecules are highly elongated. Dividing flow rate by the device cross-sectional area gives a mean fluid velocity of 0.077 mm/s within the channel. In this 15 centipoise viscosity solution, the relaxation time of

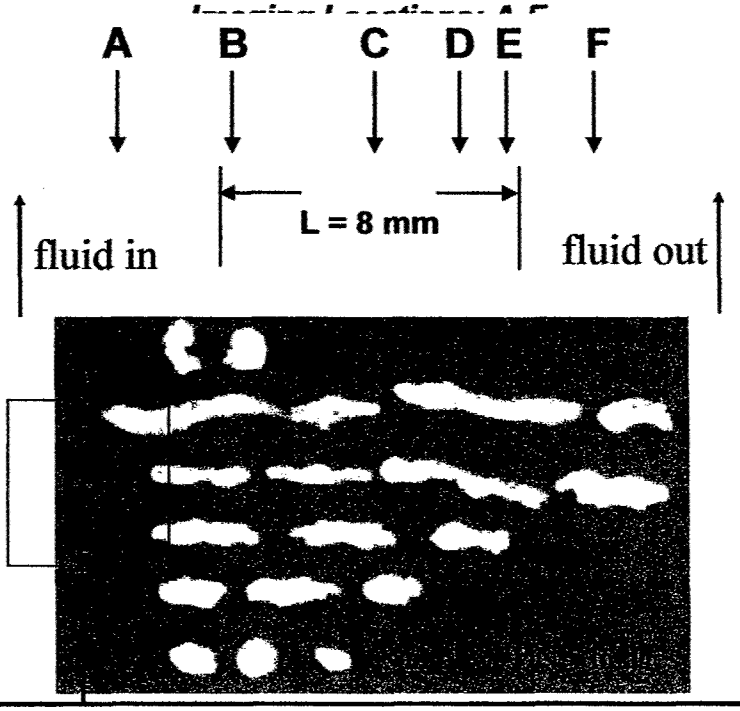

Fig. 3: λ-DNA in Elongational Flow

the molecule is 0.682 s. Therefore, in traveling 0.053 mm along the centerline, only about one relaxation time will have elapsed, and a significant fraction of the elongational stress from entering the channel will not yet have relaxed. At position **C**, the approximate midpoint of the 8 mm channel, the DNA molecules as seen in the sample images are still not entirely relaxed. Greater relaxation of the molecule is observed further downstream of the channel entrance, at positions **D** and **E**. Not until the molecule exits the channel at **F**, however, does the molecule recover the conformation observed at **A**.

A histogram analysis tracking the length distribution of a minimum of 100 molecules at each position (not shown) supports the above qualitative findings. As seen in the sample images in Fig. 3, the DNA molecules elongate in the extensional flow at **B**. Only after exiting the channel at **F** do the molecules return to a relaxed, coiled conformation observed in the device entrance reservoir at **A**. As previously, fluorescent beads were imaged under identical flow conditions experienced by DNA molecules to ensure optical streaking did not bias the measurements.

In an actual microsystem, the concentration of macromolecules in solution will vary depending upon the composition of the test sample and on the processing stage. For viscoelastic polymers such as DNA, the properties of the bulk solution are dependent upon concentration. Therefore, in order to adapt a conventional laboratory protocol to the microscale an understanding of this dependence, and of any manifestations of it in terms of solution behavior, is critical. Accordingly, we extended our previous analysis to more concentrated solutions of λ-DNA molecules.

Using an identical microfluidic straight channel device and operating under identical flow conditions, we repeated our previous experiments but increased the solution concentration of λ-DNA to 28.15 μg/ml. At this concentration, $c = 0.1c^*$, where c^* is the overlap concentration. Of the total DNA in solution, only 0.15 μg/ml received a fluorescent label. Labeling this fraction of molecules avoids excess fluorescence which obscured visualization. This data suggests that while the molecules response to shear flow or mixed shear and extension is sensitive to concentration, its response to the elongational flow along the centerline is relatively insensitive to concentration changes over this range (i.e., up to $0.1c^*$).

A dissimilarity exists between the dilute and the concentrated solution data on molecular conformation at the upstream wall location and the downstream wall location. The mean molecular lengths of molecules in dilute solution decrease when traveling from the upstream wall to the downstream wall location, suggesting that a high De flow can induce irreversible molecular damage through chain scission of molecules. For the same De flow, this behavior, however, seems not to hold for the concentrated case. The mean and median molecular lengths are similar at all downstream wall locations, and resemble closely the mean and median molecular lengths recorded at the upstream wall locations. Here again, the dynamics of molecular interactions in concentrated solution differ from those in dilute solution. This observed change in behavior can only stem from the increased concentration of macromolecules in solution. The implication is that the greater number of molecules in solution act in a manner that more effectively dissipates an applied stress than dilute solutions of molecules.

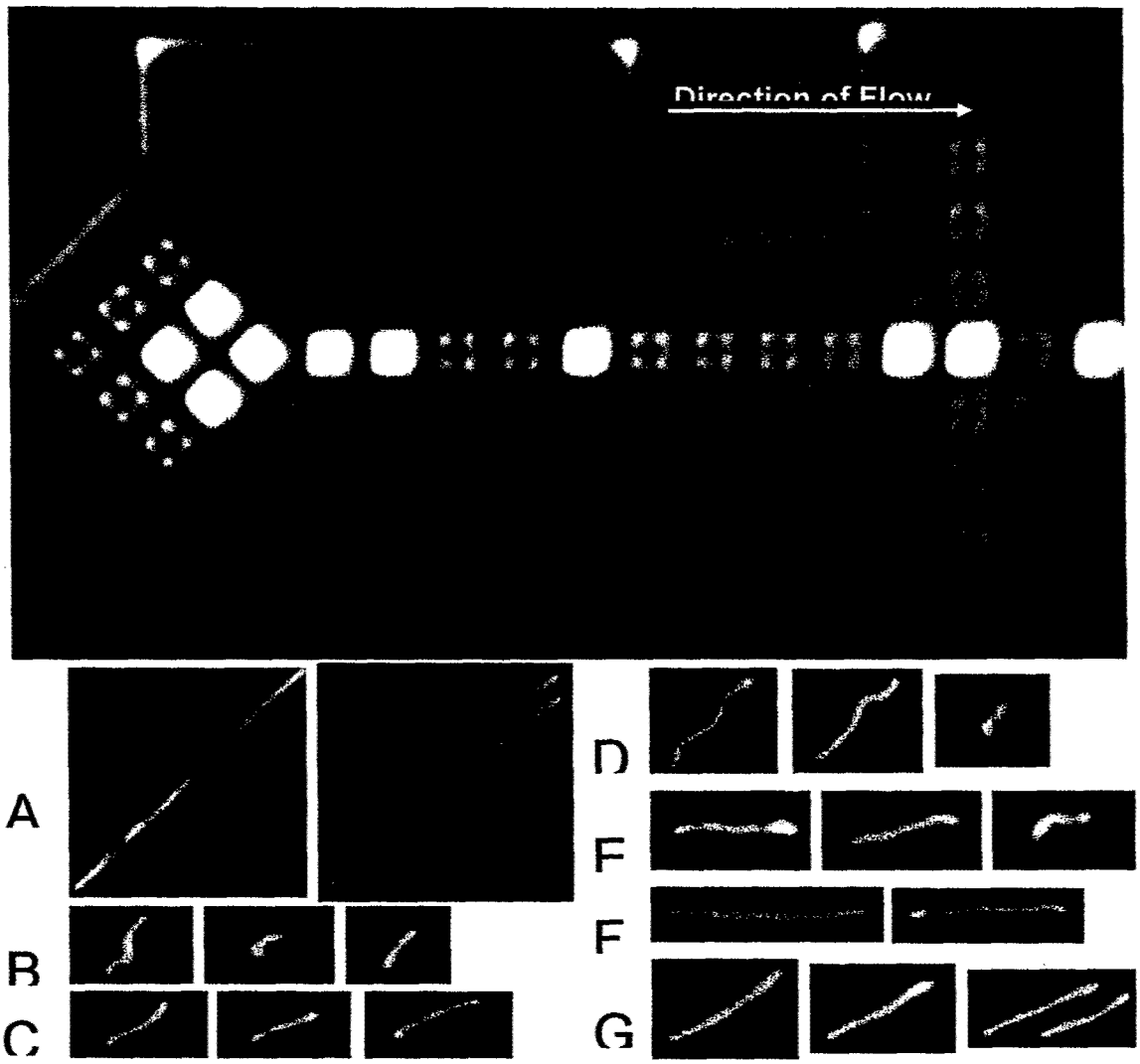

Fig. 5: λ-DNA Flow through Microcheck Valve

The extent to which device geometry and flow effects the conformation of macromolecules was investigated in a real, microfluidic device. For these experiments, λ-DNA was imaged in flow in a micro check valve. The device is entrance, marked A through G in Fig. 5. The images reveal the dramatic changes in both molecule length and orientation due to the flow. As in the straight channel experiments depicted in Fig. 3, such changes in conformation are likely to persist well downstream of the region of the flow which causes them.

The conformation of λ-DNA in both the relatively simple flow into and along a straight channel and in the complex flow in a micro check valve has been quantified using epifluorescence microscopy. In the former flow, both elongation and shear flow resulted in dramatic stretching of the molecules. The elongational flow along the channel centerline caused remarkably persistent changes in the molecule length: once stretched, the DNA was slow to relax back to the coiled state. In the high shear rate flow near the channel walls, these preliminary studies suggest that irreversible chain scission may be

occurring. Visualization in the micro check valve suggests the importance of these effects in real devices. Both conformational changes and chain scission will affect the response of the macromolecules to local sensors or processing steps, and warrant further study.

Blood Flow Experiments and Modeling

Medical micro-assay systems are being developed to perform rapid clinical chemistry using minimal sample sizes. Such systems will vastly improve medical diagnosis and patient monitoring by eliminating the often slow and cumbersome processes of conventional clinical laboratories. The basic operations of these minature assay devices will involve the transport and manipulation of blood and blood components at dimensions of tens to hundreds of microns and in volumetric rates of around 1-10□l/sec.

There are several concerns when modeling blood flow in MEMS devices. One concern is that blood cells may lyse in the extreme shear flows that can occur in these systems due to large surface-to-volume ratios in micro-channels and the channel geometries themselves (see bent and sudden contraction channels in Figure 1, for example). Lysing can be good for some situations like DNA analysis, but bad for others like quantifying potassium levels, for example. Furthermore, blood is difficult to model because it is (1) non-linear in the way shear stress depends upon shear rate, and (2) the size of red blood cells is comparable to the size of the channels in these systems.

Development of various microfluidic components to process blood in these devices must be based on a firm understanding of its non-Newtonian properties at these dimensions. This understanding will permit determination of fluid flow resistances within fluidic components as well as quantification of the high fluid shear forces incurred on blood constituents in flows through irregular geometries. It has long been established that blood is "shear thinning": viscosity decreases as shear rate increases. But while many constitutive equations have been demonstrated for blood, the validity of existing models for different flow geometries at the microscale—where the continuum assumption becomes tenuous—remains untried.

Existing models for blood can be categorized as either some variation of the power law equation or as some Casson-like equation. Both types model the dependence of blood viscosity with respect to shear rate, and Casson-like models even account for non-zero yield stresses, stresses that must be exerted before blood will shear. However, yield stresses for blood are observed only with static or low shear experiments. Based on the expected flow rates and dimensions of microfluidic components, the shear stresses generated in these devices will be very high, far exceeding the hypothesized yield stresses for blood. When yield stress is negligible, most Casson-like models simplify to some form of the power law. This study will therefore evaluate the use of the power law model to represent blood flow in prospective micro-flow geometries by comparing measured fluid mechanical resistances in these flow geometries with the flow parameters predicted from numerical simulations of the power law constitutive equation. The specific objectives of this study are: 1) to measure pressure drop versus volumetric flow rate for blood flow through channels with the following traces: 200μm x 60μm straight, 200μm x 60μm to 100μm x 60 μm sudden contraction, and 200 μm x 60μm sudden, 90° bend; and 2) to numerically compute pressure vs. flow rate relations for these flow configurations based on simulations of flow of a power law model for blood.

The channels for flow testing were fabricated in silicon using deep reactive ion etching (DRIE) to create rectangular cross-section trenches. (Fig. 1) Straight channels, channels with sudden contractions, and channels with 90° bends were all were etched 60μm deep into the silicon and had total lengths of 12mm, regardless of configuration. Both the straight channel and 90° bend were patterned with 200μm widths, while in the channel with sudden contraction, a 200μm wide, 6mm long channel fed into a 100μm wide, 6mm long channel.

(a) Top view of channels: straight, bend, and contraction

(b) Electron micrographs

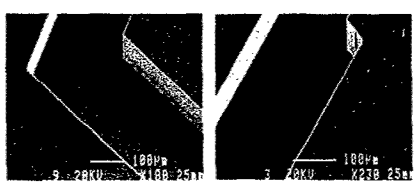

Fig. 1 Flow structures. (a) Channel configurations include straight channels, 90° bends, and sudden contractions. (b) Micrographs of bend and contraction channels.

From the earlier discussion, the constitutive equation chosen for this study was the power law equation, which has the form:

$$\tau = k(\dot{\gamma})^n$$

The specific parameters for blood (defibrinated sheep blood of 41% hematocrit) used in this study were determined from a least squares fit of the log-log relation between shear rate and shear stress, which was complied from direct viscometry of the blood. The viscometry was performed by a Vilastic 3 Viscoelastic Analyzer (Vilastic Scientific, Inc.), which measures fluid parameters of a sample as it is oscillated in a small tube.

To provide a comparison between an established constitutive model and the model formulated specifically for this study, simulations of blood flow through the straight channel and channel with 90° bend were also performed using the "one variable" power law of Walburn and Schneck, which had the parameters n=0.785 and k=0.0134 Pa•s^n, obtained at 37°C. The Walburn-Schneck model has a greater degree of non-Newtonian character than the power law model developed in this study.

Defibrinated sheep blood is a shear thinning fluid, with the viscosity dropping form 5.4 x 10^{-3} to just under 4.9 x 10^{-3} Pa•s over the shear rate range of 80 to 400s^{-1} (Fig. 2). These values are comparable to the measurements of blood viscosity in the literature. Least-squares linear fit of the shear stress vs. shear rate yielded the values for the power law parameters: k = 0.00733 Pa•s^n, and n = 0.932. These values were used in the CFD

simulations. Based on these parameters, this blood is only weakly non-Newtonian, especially at high shear rates.

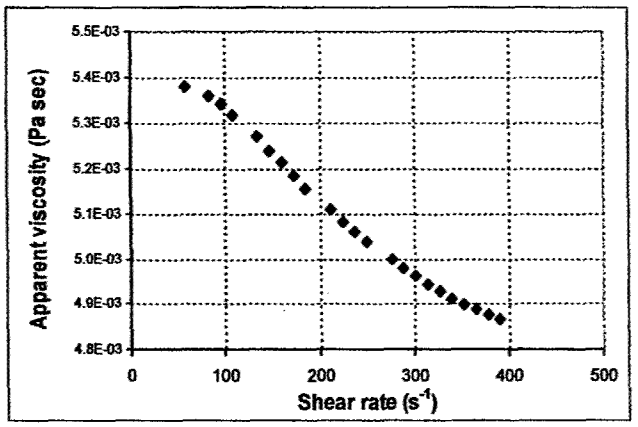

Fig. 2. Dependence of blood viscosity on shear rate. Direct measurement of blood viscosity was performed on a oscillating tube microrheometer. The measurements of blood viscosity corresponds to power law parameters of k=0.00733 Pa•s^n and n=0.932.

The pressure vs. flow rate relationships for all of the channel configurations were roughly linear, though the flow resistances were somewhat higher for lower flow rates than for higher flow rates, as would be expected for a shear thinning fluid. For the 200μm x 60μm x 12 mm straight channel, the first-order estimation of flow resistance for blood was about 1.3 x 10^{13} kg/(s•m^4) roughly 3.5 times that for water. The addition of the ninety degree bend midway through the channel increases the flow resistance to about 1.8 x 10^{13} kg/(s•m^4), while with a sudden contraction midway and subsequent width reduction to 100μm, the flow resistance was about 2.5 x 10^{13} kg/(s•m^4).

Steady state flows of both the power law models and a Newtonian reference were numerically simulated for each of the flow geometries by the CFD-ACE+ CAD suite of software tools, a pressure-based, finite volume flow solver. Using the chosen power law flow, the simulation was perfomed with explicit volumetric flow rates, and resulting pressure generated between inlet and outlet of the flow structure was computed. These simulations produced pressure vs. flow rate relationships that were similar to the trends and magnitude of experimentally determined relationships. As with the experimental measurements, the computed relationships between pressures vs. flow rates were roughly linear. With both the straight channel and the channel with sudden contraction, results of numerical simulations closely matched the experimental measurements (Fig. 3a,c). Simulations of the flow through the channel with the bend, however, predicted pressure drops that were consistently smaller than the pressure drops measured during flow experiments (Fig. 3b).

Not surprisingly, simulations using the Walburn-Schneck model for blood flow through the straight channel and channel with bend produced pressure vs. flow relationships that deviated more from linear than relationships produced with our power law model. Hydrodynamic resistances (slopes in Fig. 4) were visibly lower for higher flow rates than they were for lower flow rates. Overall, the flow resistance were much lower for the

Walburn-Scheck model than for our model, since the high shear viscosity predicted the former are much lower.

(a) Straight channel: 200μm x 60μm x 12mm

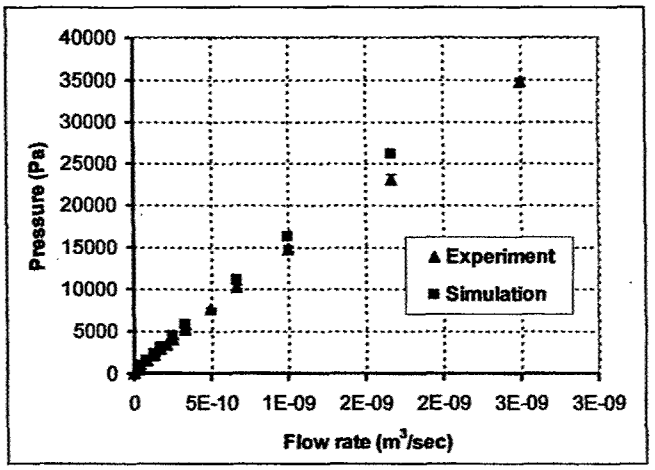

(b) Bend: 200μm x 60μm x 6mm → 90° bend → 200μm x 60μm x 6mm

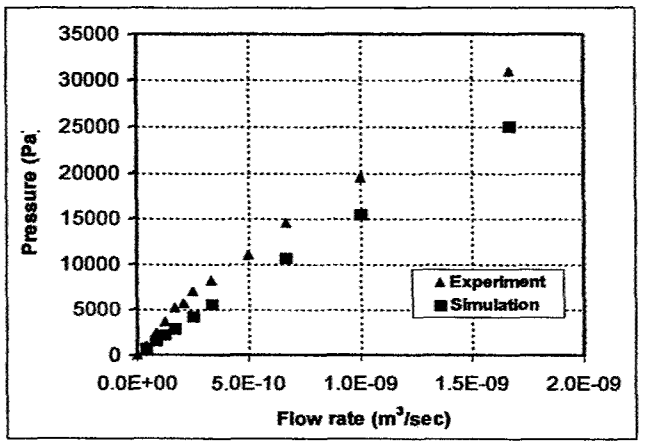

(c) Sudden contraction: 200μm x 60μm x 6mm → 100μm x 60μm x 6mm

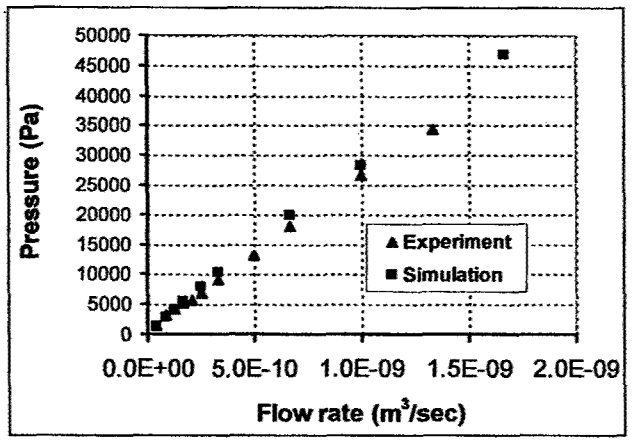

Fig. 3. Pressure vs. flow rate relationships. Both experimental measurements and simulation results with our power law model are shown.

(a) Straight channel: 200μm x 60μm x 12mm

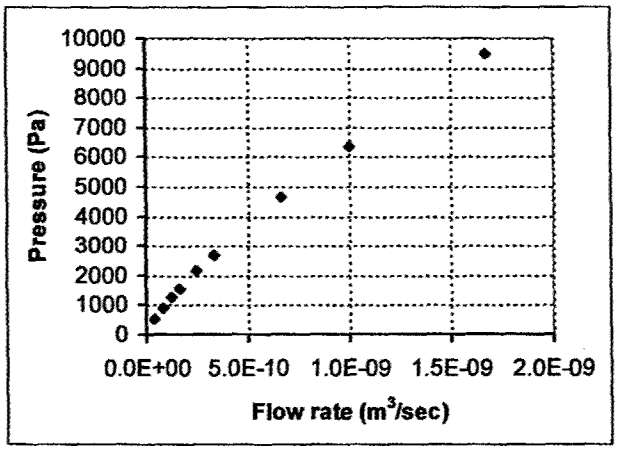

(b) Bend: 200μm x 60μm x 6mm → 90° bend → 200μm x 60μm x 6mm

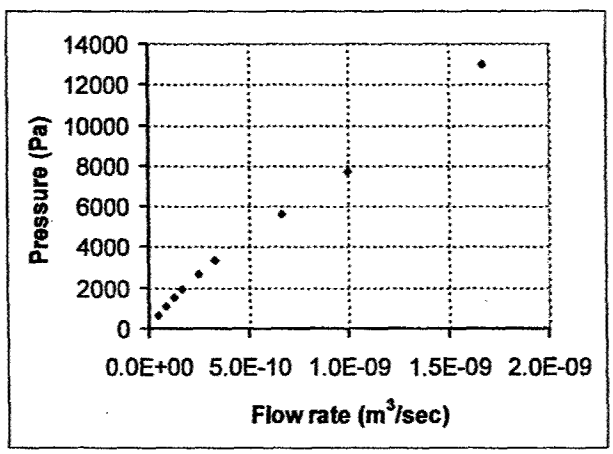

Fig. 4. Simulations of pressure vs. flow rate relationships using the one variable Walburn-Schneck power law.

While this study is among the first to explicitly measure flow parameters of blood in microfabricated devices, it is merely a prelude to more rigorous studies, which will examine the microstructure of flows through a greater variety of geometries and scales. This study considered only the whole hydrodynamic *resistances* of three simple channel geometries. Future studies will map velocity and shear rate profiles within the flow geometries. More advanced work will even account for expected changes in local hematocrit in various flow geometries. Additionally, it will be important to observe the orientation, deformation and hemolysis of blood cells subject to different flow conditions involving high shear rates. The knowledge obtained from these studies set important guidelines for designing and configuring various microfluidic devices to support development of lab-on-a-chip assay systems.

Publications

Trebotich, D., Zahn J. D. and Liepmann D. (2002), "Complex Fluid Dynamics in BioMEMS Devices: Modeling of Microfabricated Microneedles," Technical Proceedings of the 2002 International Conference on Computational Nanoscienceand Nanotechnology, and Technical Proceedings of the Fifth International Conference on Modeling and Simulation of Microsystems, April 22-25, San Juan, Puerto Rico.

Chang W.C., Liepmann D, Lee LP. (2002). "Biomemetic Cell Sorting with Selectin Proteins," Proceedings of the Materials Research Society Volume 729, 2002 MRS Spring Meeting, April 1-5, San Francisco.

Stoeber, B. and D. Liepmann. "Design, fabrication, and Testing of a MEMS Syringe." Proceedings of Solid-State Sensor and Actuator Workshop. 2-7 June, 2002, Hilton Head Island, SC, Transducers Res. Found (TRF Cat. No.00TRF-0001).

Chang WC, Liepmann D, Lee LP. (2002). "A biomimetic method for extracting leukocytes from blood in microfluidic devices." Proceedings of the 2nd Annual International IEEE-EMBS Special Topic Conference on Microtechnologies in Medicine and Biology (Cat. No.02EX578), Madison, WI, 2-4 May 2002,184-8

Shrewsbury P.S., Muller, S.J., and Liepmann, D.(2002), "Effect of Flow on Complex Biological Macromolecules in Microfluidic Devices," *Biomedical Microdevices* **4**: 17-26.

Trebotich, D., Chang, W. and Liepmann D. (2001), "Modeling of blood flow in simple micro-channels," Technical Proceedings of the Fourth International Conference on Modeling and Simulation of Microsystems, Hilton Head Island, NC, March 19-21, 2001, pp: 218-222.

Dickey, C.K., Makhijani, V.B., Deshmukh A. and Liepmann, D. (2001) "Computational Design Analysis for In-Plane Microfluidic Valves," Technical Proceedings of the Fourth International Conference on Modeling and Simulation of Microsystems, Hilton Head Island, NC, March 19-21, 2001, pp: 235-238.

Liepmann, D. (2001) "Microfluidics for Delivery of Reagents," Photonics West 2001: International Biomedical Optics Symposium (BiOS), Proceedings of SPIE Vol. 4265, Paper No. 4265-05.

Liepmann, D., (2000). "Drug Delivery, Microfluidics, and MEMS." Proceedings of ICMMB-11: International Conference on Mechanics in Medicine and Biology, Maui, Hawaii, April 2-5, 2000.

Shrewsbury, P. J., Muller, S. J. and Liepmann, D. (2000). "Flow of lambda -DNA in microfluidic devices". 1st Annual International IEEE-EMBS Special Topic Conference on Microtechnologies in Medicine and Biology, Lyon, France, 12-14 Oct. 2000, 415-20.

Chang, W., Trebotich, D., Lee, L. P. and Liepmann, D. (2000). "Blood flow in simple microchannels". 1st Annual International IEEE-EMBS Special Topic Conference on Microtechnologies in Medicine and Biology, Lyon, France, 12-14 Oct. 2000, 311-15.

Zahn, J.D. and Liepmann, D. (2000) "Complex Biological Fluid Flow Through Microfabricated Microneedles," *Proceedings of the ASME MEMS 2000 Symposium*, November 2000.

Shrewsbury, P. J., Muller, S. J. and Liepmann, D. (1999). "Characterization of DNA flow through microchannels". International Conference on Modelling and Simulation of Microsystems, Semiconductors, Sensors and Actuators, San Juan, Puerto Rico, 19-21 April 1999, 578-80.

Lee, L.P., Berger, S.A., Ferrari, M. and Liepmann, D. (1999) Fabrication of Fluoropolymer Based Microphotonic Components for Biomedical and Environmental Applications," Photonics West 1999: International Biomedical Optics Symposium (BiOS) Conference, Jan. 23-29, San Jose, CA, Proceedings of SPIE Vol. 3606, paper # 3606-20